Study the Interaction between Hydrophilic Silica Surface and Planar DMPC Bilayers by Using Molecular Dynamics

By

Ting Li

A thesis submitted to the

Graduate School-New Brunswick

Rutgers, The State University of New Jersey

In partial fulfillment of the requirements

For the degree of

Master of Science

Graduate Program in Chemical & Biochemical Engineering

Written under the direction of

Dr. Aleksey Vishnyakov

Dr. Alexander V. Neimark

And approved by

_____

_____

_____

New Brunswick, New Jersey

January, 2016

ABSTRACT OF THE THESIS

Study the Interaction between Hydrophilic Silica Surface and Planar DMPC Bilayers by Using Molecular Dynamics

By Ting Li

Thesis Director:

Professor Alexander V. Neimark

Professor Aleksey Vishnyakov

This work studies the interaction of lipid bilayer with hydrophilic silica surface. Main attention is paid to the dependence of the disjoining pressure Π on the distance between the bilayer and the silica substrate h. Π is calculated as a force that compensates the external gravity–type force applied to the bilayer per unit surface area. The dependence of the disjoining pressure on the distance deviated from the expected sigmoidal shape, showing at least two types of stable configurations with negative (attractive) Π . Structure and the mobility of lipids in the bilayer, as well as the water in the gap between the bilayer and the substrate were characterized by lateral diffusion coefficients, order parameter, hydrogen bond numbers as well as radio and spatial distribution functions.

TABLE OF CONTENTS

ABSTRACT OF THE THESIS ii

1. Introduction 1
- **1.1 Experimental method to study SLBs** 2
- **1.2 Simulation studies of self-assembled lipid mono- and layers with external surfaces.** 12
- **1.3 Goals of the present work** 16

2. Simulation Methodology 17
- **2.1 Molecular Dynamics simulations** 17
- **2.2 Force Field** 18
- **2.3 Building the model of silica substrate** 20
- **2.4. Simulation details** 21

3. Results 23
- **3.1 SLB – Substrate Interaction Force** 23
- **3.2 Characterization of the Structure** 31
  - 3.2.1 Orientation of Phosphatidylcholine Headgroups 31
  - 3.2.2 Order Parameters 32
  - 3.2.3 Diffusion coefficient of water 34
  - 3.2.4 Hydrogen Bond 36
  - 3.2.5 Radial Distribution Functions 37

4. Conclusion 40

5. References 42

1. Introduction

Supported Lipid bilayers (SBL) play an important role in many areas [1-7]: In particular, they are employed as simplified model systems for studies aimed at improving the understanding of the properties and functions of biological membranes. SLBs, being essentially immobilized, allow investigations with broad spectrum of experimental characterization techniques which seems hard apply to actual cells or freestanding lipid bilayers, such as atomic force microscopy (AFM), surface force apparatus (SFA), quartz crystal microbalance with dissipation (QCM-D). Knowledge of structure and thermodynamics of SLBs is important for understanding of cell interactions with solid supports and drug delivery applications[5].

Lipids commonly assemble into SLBs on hydrophilic surfaces and moderately hydrophobic surfaces, such as silica glasses and mica. Typically, an SLB does not contact the supporting surface but there exist a confined water layer of 6~15A in thickness between membranes and solid supports [1, 8-12]. It has been reported that the molecular structure of water layer, as well as the structure and properties of SLBs are affected by the substrate [11, 13-16], and therefore depends on the substrate material and functionalization of the surface.

From the thermodynamic point of view, the effect of the substrate on the structure of properties of the bilayer and the solvent film between the bilayer and the substrate should be interpreted in terms of the free energy. The free energy of SLB – substrate interactions may be presented as the sum of dispersion forces, long-range electrostatic forces, and

solvation forces. Dispersion forces are short-range forces arising from van de Waals interactions acting between membranes and substrate. They are strong and repulsive on short distances, weak and attractive on longer distances between the substrate and bilayer. They steeply decay to zero as the separation between the SLB and the substrate increases. Electrostatic forces are strong and long-range. They result from the surface charge on both substrate and SLB The surface charge may originate from the ionization or dissociation of surface groups (e.g., hydroxyl group of hydrophilic silica substrate can be dissociated as –O- and H+, which leads the surface charge as negative). Many lipids are also ionic (at least in a particular range of pH) or zwitterionic. Solvation forces are also known as disjoining forces or hydration forces. They are caused by the dependence of the liquid structure and thermodynamics of solvent film between the SLB and substrate. As the liquid solvent tend to be "reordered" near the surfaces due to interactions with various functional groups of the SLB or the substrate.

The effective force between the surfaces is calculated as the derivative of the free energy by the distance. Taken per unit surface area, this force called the disjoining pressure [17]. SLB interactions with various substrates were extensively studied both experimentally and theoretically and a short review of such studies is given below.

1.1 Experimental method to study SLBs

SLBs are obtained by Langmuir – Blodget deposition technique or by vesicle spreading. Surface force apparatus (SFA) and atomic force microscope (AFM) are most popular experimental techniques for studying the total interaction pressure of two surfaces [18-23]. In SFA, two cylinders are slowly brought into a contact and the force between them

is measured as a function of the distance. Because mica is easily coated by lipids SFA has been widely used for measuring the interaction forces between different lipid-coated surfaces [22-26]. The examples include forces between two SLBs [22, 27], forces between SLB and uncoated mica [24-26], as well as the interactions between self-assembled lipid monolayers on hydrophobic supports with SLBs [23] or mica [28]. A number of studies are focused on the forces between hydrophilic substrates and SLBs. For example, Anderson et al investigated the formation of DMPC bilayer on various silicate glass surfaces in various aqueous solutions and measured the surface forces with SFA. The schematics of SLB adhesion and the dependence of the surface force on SLB—substrate separation are shown in Fig 1-1-1-B. [24] It should be noted that the $f(D)$ profiles reflect both SLB interactions with the substrate and SLB interactions with the mica cylinder. Often, the $f(D)$ on approach (D decreasing) differs dramatically from $f(D)$ observed on reproach (D increasing). In ref [24] the force on approach is repulsive and increases monotonically as D decreases. On the way back, when the separation increases, strong adhesion forces are observed. This hysteresis is due to difference in bilayer geometry on approach and reproach: at the same D the distance h between the SLB and the substrate is actually different because of the adhesion between the SLB and mica (shown as Fig.1-A). And this adhesion may mainly come from the electrostatic effect between them, despite the fact that overall the SLBs is not charged.

A B

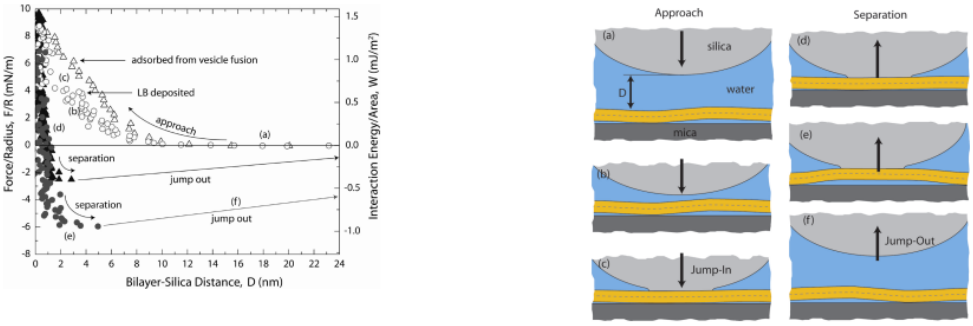

Figure 1-1-1. A) Force-distance profiles of silica-different prepared supported DMPC bilayer interaction: triangle-DMPC bilayer prepared on mica by vesicle fusion; circles-bilayer prepared by deposition. B) Schematics of the detecting process. (a) Surfaces are driving closer to each other by constant velocity. (b) The silica feels an initial repulsion due to repulsive undulation and hydration forces. (c) The repulsive barrier is over- come, and the surfaces jump into adhesive contact. (d, e) The surfaces are pulled apart but stay in adhesive contact as the force measuring spring is decompressed. (f) The spring force equals the adhesion force and the surfaces jump apart.

Valtiner et al[23] measured the forces between self-assembled monolayer (SAM) functionalized with different terminating groups and lipid bilayers coated Short hydrophilic DSPE-PEG polymer chains terminated by ammonium nitrate groups were attached to the bilayer surface (shown as 1-1-2). The polymers provided an entropic repulsion force between the bilayer and the SAM surface. –COOH or $–CH_3$ head groups were attached to the SAM, the force-distance profile showed a strong attractive adhesion force, but for –OH head group, there was no significant adhesion force. Comparing the different force-distance curve, the author concluded that with alcohol termination groups, the SAM surface was hydrophilic and offered no specific binding sites for headgroups of bilayers. The dominant forces are repulsive steric polymer and weak attractive van der Waals forces; For –COOH terminated SAM, specific acid-base interactions between the basic ammonium and acidic carboxyl groups lead to a significant attraction forces when two surface separating; For $–CH_3$ terminated SAM, hydrophoic attraction forces leads a much stronger adhension forces than –COOH terminated SAM forces.

A

B

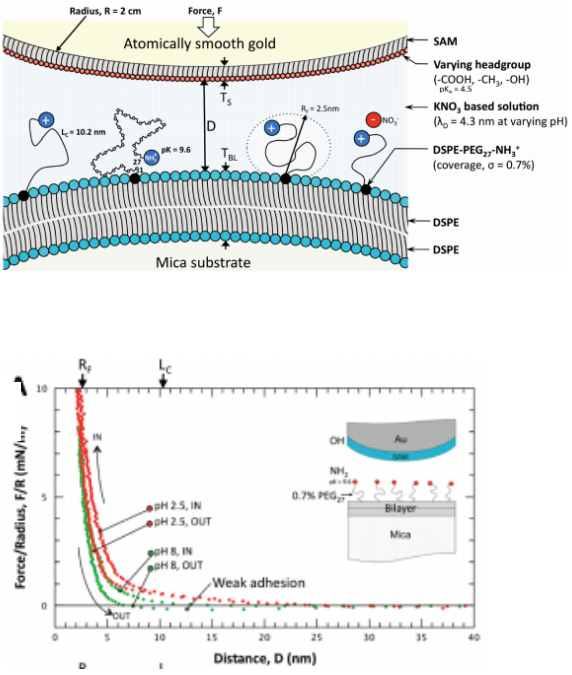

Figure 1-1-2 A) Schematic of the experiment and surface modifications. B) Force–distance profiles between end-functionalized PEG_{27}-NH_2 surface and an alcohol (OH) terminated SAM surface in KNO_3 based aqueous solutions with an ionic strength of 5 mA at pH 2.5 and pH 8 measured. At pH = 2.5 both approach and separation are purely repulsive because of the steric repulsions of the end-grafted PEG coils and hydration forces. At pH = 8 the approach is repulsive but the separation shows a weak adhesion.

Also many studies have been conducted to measure the interaction between hydrophobic or hydrophilic monolayer and mica or hydrophobic monolayer [23, 25, 26, 28]. These systems do not involve supported bilayers. However, since the surface structures of the monolayers and bilayers are similar, the resulting forces are also relevant to our study. Furthermore, monolayer systems may include only one water layer while the SFA studies of SLBs have to deal with two. For example, Yu[26] measured the force-distance profile between mica and SAM deposited on gold. In the gap, the authors placed a thin layer of mussel foot proteins. The degree of hydrophobicity of the protein layer was manipulated via pH that changed from acidic pH=3 to slightly basic conditions pH=7.5. PH increase weakened the hydrogen bonding between the protein layer and the SAM. Strong adhe-

sion was observed only at acidic conditions, when specific binding between proteins and the SAM caused by strong hydrogen bonds was present. At basic conditions, the adhesion was practically eliminated. One may conclude that in neutral solution, the adhesion forces between two hydrophilic surfaces cannot be very strong.

Generally, when not considering the specific bonding "bridge" between head group of membranes and surface groups of solid support, or fusion effect between lipid layers, the detected force-distance curve can be explained by electrostatic, van der Walls and solvation forces mentioned above. Long-range repulsion forces at long distances mainly account for the electrostatic force between the double electric layers formed at the surfaces. On shorter range, solvation force also becomes repulsive. Adhesion (that is, an attraction to the substrate) is caused at shorter distances by strong hydrophobic interaction[25] and/or electrostatic attraction between neutral lipids layer and charged solid surfaces[24]. Finally, at very short distances a strong repulsion between SLB and substrate is caused by solvation force and short-range dispersion repulsion. As a result, the dependence of the effective force between the substrate and bilayer often has a sigmoidal shape that will be discussed in details below.

Though SFA has a very widely application on measuring the interaction forces between two bodies, it has its own limitation. First, low lateral resolution-the normal distance resolutions can be 0.1nm; second, SFA cannot measure the molecular composition and structure directly. [29].

Another technique widely employed for studies of SLB-substrate interactions is Atomic Force Microscopy (AFM). In principle, AFM is similar to SAF, but AFM measures the forces between a fine tip and a sample surface. This means that instead of

macroscopic surfaces, the samples can be manipulated at nano scale. Forces-curve collected by AFM can supply information about physical and chemical properties of the sample, such as the nature of surface functional groups or local effect of the liquid medium. Fig 1-1-3 schematically demonstrates an interpretation of force-distance curves for AFM probing of SLBs.

The approach – reproach hysteresis characteristic to SFA is also observed in AFM. Generally the force-distance curves obtained on the tip approaching and retracting are very different, and they also give different information: one is approaching curve, another is retracting curve. They can offer the very different information: for approaching parts, the curve can be used to characterize surface forces by detect the force curves under different solutions with different PH or ionic concentration —including van der Waals and electrostatic forces[21], solvation forces[30, 31], hydration forces[21]. When the cantilever begins to penetrate the layer, mechanical properties of the sample can be obtained [32-34]. For the retracting process, the adhesion forces can be measured [35, 36].

A B

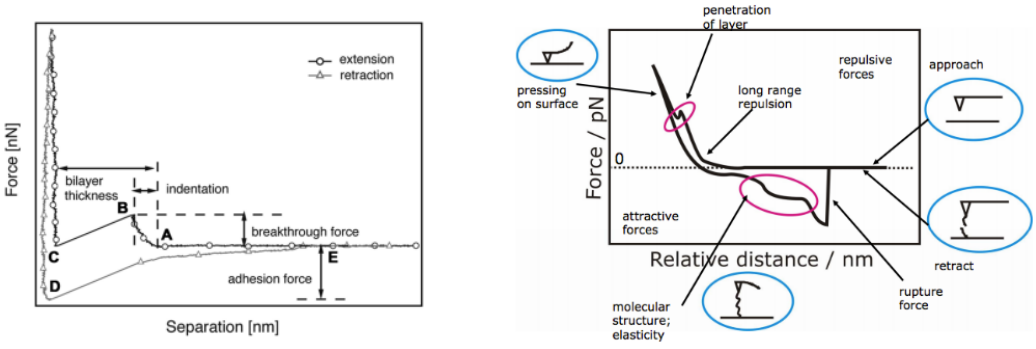

Figure 1-1-3. A) Generally force curve detected by AFM. B) Schematic of AFM detected process.

Several attempts have been reported using AFM to sample the properties of different architectures of supported membranes by using either bare tips or modified tips [37-42]. Chinmay et al detected the force-distance curves by attaching AFM tip to dioleoyl-phosphatidylcholine (DOPC) - egg sphingomyelin (SM) - cholesterol (CHOL) phase separated supported bilayer. For the different composition ratios of conponents, the system can be spontaneous separated as two phases:: one is SM rich phase with relative thick and ordered tails, one is DOPC rich phase with relative thin but disordered tails. Different force-distance got from these two phases: For DOPC rich bilayer, the force curve can be fit to mean square equation, however, for SM rich bilayer, there will be two distinct elastic regions separate by a crossover area. They attribute this difference to the formation of inner hydrogen bonds in SM rich membranes, which may also deform the phase to an ordered state [37]. With hydrophilic and hydrophobic monolayer modified mica tip, Schneider et al measured the interaction between the tips and four kinds of SBLs with different head groups-differ from hydration ability. When using –OH terminated tip, the force-curves generally have relative strong repulsion forces, which are generally contributed by the combination of mechanical and hydration forces. And also the profile is sample dependents. However, when turns to $–CH_3$ modified AFM probes, the breakthrough forces of all materials are near zero. The main different between the two probes can be explained as below: the $–CH_3$ stabilize the intermediate, reducing the breakthrough force; In other words, the hydrophilic tip change the structure of intermediate, cause an increase of repulsion force on the approach process [38]. Many studies also focus on the interaction between SLBs and SLBs [39-42] Israelachvili identified the forces dominated the interaction of two bilayers. The attractive force is really weak, which is dominated by van

der Waals force, the dominates of repulsive forces are not clear: either from hydration forces, which arising from the reconstruction of water layer effected by the head group of bilayers, or from entropic “protrusion” effect, contributed to the roughness of molecular roughness [43]. In Pera’s paper [42], they measured the forces-distance curves under three different kinds of systems: planar SLBs with bare silicon tips, planar SLBs with bilayers modified silicon tips, bare mica surface with bilayer modified tips. When compared the force-distance curve of these systems, one can found that the retraction curves are quite different: Long range attraction can be observed in bilayer-bilayer force profile, a possible explanation is that a bilayer tether formed between the surface and tip (shown as Fig 1-1-4-.F). The tether’s formation which can also been explained as hemi-fusion, which was also observed Donaldson by using SFA [27]; Interaction between tip-bilayer and bilayer-planar surface is very different （Comparing Fig 1-1-4-A and Fig 1-1-4-G）. For Fig 1-1-4-G to Fig 1-1-4-I, there is no clearly explanation for the long-range large attractive force. The hydration of membranes, as well as the hydration of solid surfaces has been studied by many researchers [8, 44-49], shows that there do exist several confined water layers either near the membrane surface, or near the hydrophilic solid surface. But almost no experimental literature gives any insights about how interface water interplay between the bilayer and support.

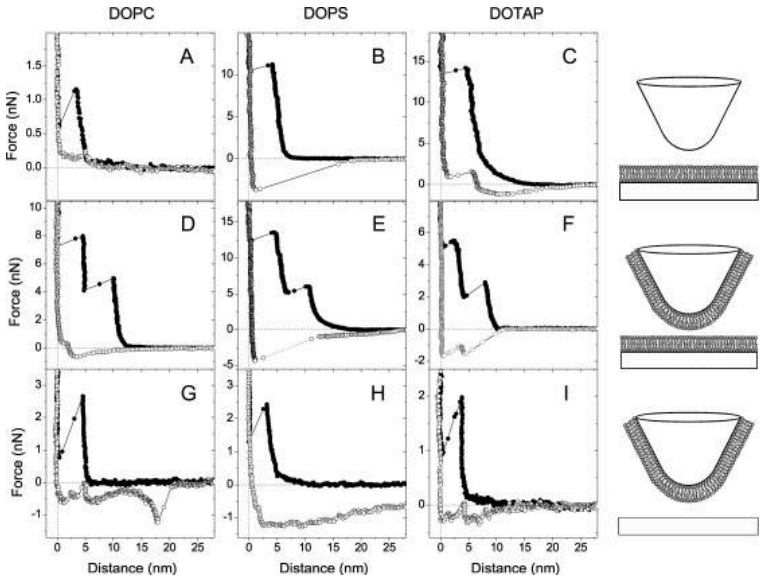

Figure 1-1-4. Typical force-versus-distance curve measured on a planar mica surface with a bare silicon nitride tip in buffer after exposure to (A) DOPC (radius of curvature of the tip R 1⁄4 45– 50 nm), (B) DOPS (R 1⁄4 100–150 nm), and (C) with DOTAP (R 1⁄4 200–250 nm) vesicles. The schematic on the right shows our interpretation of where bilayers are adsorbed. Force curves obtained with a mercapto undecanol ($HS(CH_2)_{11}OH$)-gold coated tip on mica after exposure to (D) DOPC (R 1⁄4 45–50 nm), (E) DOPS (R 1⁄4 100–120 nm), and (F) DOTAP (R 1⁄4 100–120 nm) vesicles. Typical force curves obtained with a mercapto undecanol- gold coated tip on a planar mercapto ethanol ($HS(CH_2)_2OH$)-gold surface after exposure to (G) DOPC (R 1⁄4 60– 65 nm), (H) DOPS (R unknown), and (I) DOTAP (R 1⁄4 70–75 nm) vesicles.

The forces acting between the probe and the tip measured in AFM, also result from both interactions between tip and bilayer and from the interaction between the SLB and the substrate, similarly to SFA experiments. AFM however can be set up to study the interaction of the tip with a freestanding lipid bilayer (FLB). The experimental setup is shown in Figure 1-1-5-A. The bilayer membrane is stretched on a support with a hole drilled though. Over the opening, the bilayer membrane approximates FSB, although the diameter of the hole still matters and affects the bilayer membrane interaction with the tip (Fig 1-1-5-B). The $f(D)$ dependence shows a wide hysteresis caused by spontaneous adhesion of the membrane to the tip. The bilayer deformation and the force allow probing both adhesion and the mechanic properties of the bilayer, elasticity in particular. [32, 50,

51]

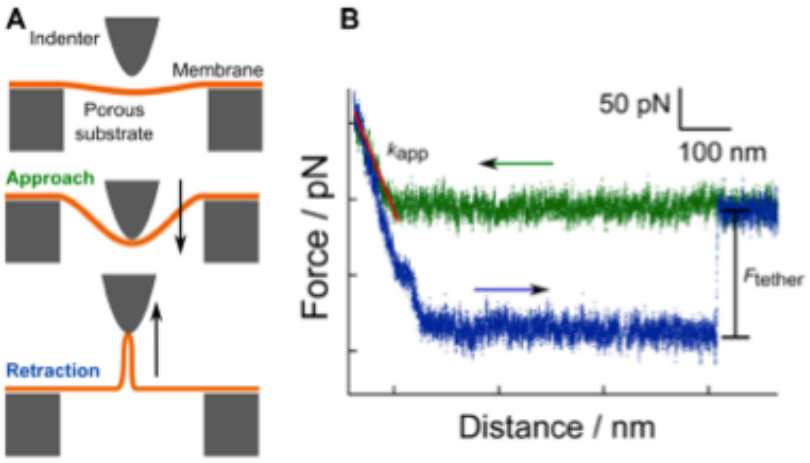

Figure 1-1-5. A. Schematic drawing of a force cycle composed of indenting the membrane with the AFM tip upon approach and tether formation upon retraction. B. Force distance curves showing a linear force response upon indentation of the pore-spanning membrane (green) and formation of a tether upon retraction (blue) giving rise to a constant force plateau (F_{tether}). The red solid line shows the determination of kapp and the black solid line F_{tether}

On strongly hydrophobic supports, lipids adsorb in form of self-assembled monolayer (SAM). Interactions between the monolayers with the outer surfaces (that is the surface approaching SAM from the aqueous phase) are of substantial interest, because the structure of a SAM and a FSB leaflet are similar. Therefore, the solvation forces between a SAM and an approaching object should also be similar in nature to those for FSB. SAM are easier to study compared to FSB, especially with AFM, [20, 28, 52-57]. Kim studied the disjoining pressure between hydrophobic monolayer and silicon surface. He gave a picture how disjoining pressure changes with the monolayer's thickness: except an attractive force when the thickness is smaller than 60A, there is also a strong repulsion forces as the thickness increasing, which is the result of several forces- repulsion van der Waals forces between adsorbed monolayer and desorbed part, hydrophilic and hydrophobic interaction of the head groups[56]. Ma studied the interaction between alkyl-terminated

AFM tips and –SH terminated monolayers, indicated that the adhesion forces were affected most by the hydrophobic interactions between these two layers. There is no significant long-range repulsion or attraction can be observed on the force profiles, similar as other monolayer studies.

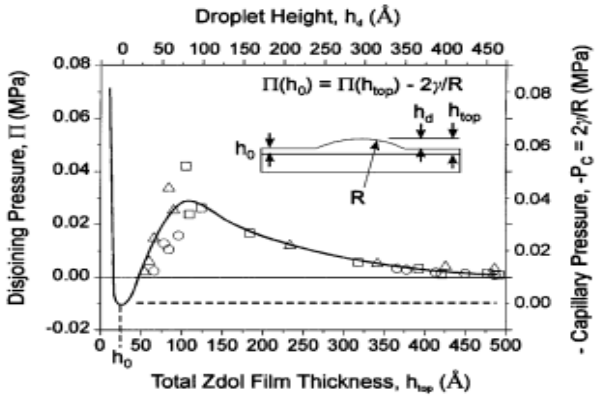

Figure 1-1-6. Disjoining pressure and capillary pressure as a function of Zdol polymer film thickness. The three different types of symbols represent AFM measurements on three different droplets as they shrink and disappear

1.2 Simulation studies of self-assembled lipid mono- and layers with external surfaces.

Molecular simulations (atomistic molecular dynamics and Monte Carlo, as well as coarse- grained techniques such as CGMD) have also been employed to study the SBLs. They mainly focus on the influence of the substrate on the bilayer structure, elasticity and dynamics. A few simulation studies target the disjoining pressure between the SLB and a substrate. Heine [58] using atomistic molecular dynamics in NVT ensemble to study how hydrophilic a-quartz influence the dynamics of the DPPC bilayer. The system was periodic in lateral directions. The main problem was that water could not freely exchange between the equilibrium bulk and the film between the SLB and the substrate (the film

thickness was 33~35A, which is in agreement with experimental measurements [59]), except through the SLB. Diffusion of water through the bilayer membrane is extremely slow, and the water transport rate was nearly zero. In order to move the bilayer to specified separate distance, the author had to specify the number of water molecules above and below the bilayer, which may lead to incorrect distribution of water. Furthermore, the rigidity of substrate decides the system cannot use NPT ensemble, and this will definitely affect the dynamics of bilayer. Such a method can be used in studies of the structural properties but not the SLB-substrate forces. Roark and Feller improved the model: they "drilled" a hole through the silica substrate, allowing water exchange between the confined film and the bulk. In this study performed under constant volume conditions, they found that the water layer between the substrate and bilayer is very narrow, and the degree of hydroxylation only has very little effect on the thickness of the layer. Their approach also has some drawbacks: first the hole was relatively wide and could affect the geometry of the bilayer; the silica model lacked some significant elements, such as the roughness of the substrate surface [60].

Monte Carlo simulations allow (1) direct particle exchange between the film and the bulk (2) control over the pressure in the bulk (3) calculations of free energies. Pertsin el al used the grand canonical Monte Carlo method to represent the interaction between gold supported DLPE bilayers and alkanethiolate self-assembled monolayers (SAMs). Both hydrophilic, COOH-terminated, and hydrophobic, CH_3 -terminated, SAMs were considered. The advantage of this method is that it can allow the interlayer water molecules to exchange with the bulk water. The pressure-distance profile was obtained and also the free energy of adhesion was calculated (shown as Fig 1-2-1). For hydrophilic substrate,

the value of free energy is 20times larger than hydrophobic substrate. The pressure measured here can be analyzed as two parts: directly bilayer-substrate pressure and hydration pressure. The reducing of adhesion potential of hydrophobic substrate is caused by the missing of electrostatic terms. In their later work, they perform the simulation to study the information between gold-supported DLPE bilayers but strong hydrophilic mica surface. [61]The interaction energy of the system has been separated as two body: one is direct bilayer-support interaction force, $\boldsymbol{f}_{\mathrm{d}}$, which only depends on the location of the bilayer and substrate; another one is hydration force, $\boldsymbol{f}_{\mathrm{h}}$, which related to the interaction of bilayer and substrate in aqueous phase. The pressure-separation profile was measured, and it can be divided into four parts (shown as Fig 1-2-1-B): For part A, the separation of bilayer and substrate is large, the mainly dominant pressure is hydration pressure, corresponds to the configuration that the choline nitrogen group of DLPE bilayer prefer to "stand-up", which means about half about the P-N vector with bilayer normal is smaller than 60^{o}, making the bilayers much easier to interact with water; For part B, the orientation of P-N vector preferentially parallel to the bilayer plane, as the consequence of interplay between hydration bilayer-water and electrostatic bilayer-mica. ; For part C, the total interaction force becomes attractive, arising from the increasing $\boldsymbol{f}_{\mathrm{d}}$, which causes by the formation of hydrogen N-H—O bond and the electrostatic attraction between phosphate group and charged mica surface; In part D, the large repulsion caused by short contacts between mica, water and bilayer. Even with a smaller separation and larger pressure, there do exist a water layer between substrate and bilayer.

A B

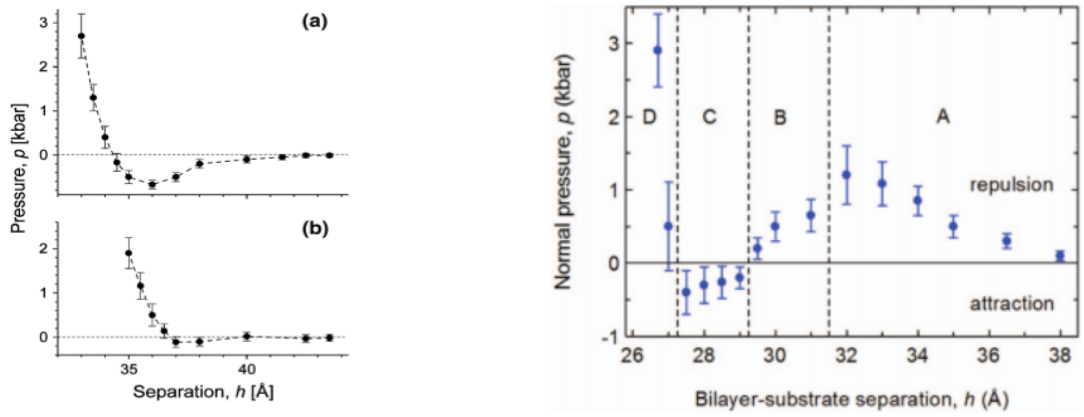

Figure 1-2-1. A) Pressure-separation profiles of DLPE and a) hydrophilic SAM b) hydrophobic SAM. B) Pressure-separation profiles of DLPE bilayer and mica surface.

Atomistic simulations of SLBs are limited because of computational expenses. The systems are always large and complicated: when we want to examine the intermolecular dynamics of the system, not only the lipids but also the substrate has to use the all-atomic force field, which makes calculations really heavy. Corse-Grain simulations overcome these limitations: several atoms of a lipid molecule are lumped together into a larger quasi-particle; thus the system is represented by a collection of a smaller number of quasiparticles, which interact via coarse-grained, simplified potentials [62] [63] The price to pay is crudeness of the potentials and many essential features or the system may be omitted as a result. The biggest concern is the structure and entropy of the solvent film between the bilayer and the substrate, which are not correctly represented by spherical Lennard-Jones models of water typically used in coarse-grained MD simulations. Xing performed a CG simulation of a big system (with system size as 12*13.2*12.7 nm^3) to study the interaction between DPPC bilayer and hydrophilic substrate [62]. They compared the

simulation results of four different situations: freestanding bilayer, SBLs with flat substrate, SBLs with rough surface, found that the existences of bilayer freeze the inner leaflet: the rougher the surface, the higher diffusion the inner leaflet has. But for the outer leaflet, the effect of substrate is very little. They also found that there exit an ordered water layer with 1nm thickness near the surface. In their later work, they calculated the lateral pressure, demonstrating that the lateral pressure become asymmetry due to the substrate, implying the membrane are under strong tension[64]. Hoopes et al also found a strong asymmetry in density and pressure[63]. However, coarse-grained MD studies just give us a view how the substrate affects the bilayer not the disjoining pressure between SLB and the substrate.

1.3 Goals of the present work

In this paper, we investigate the interaction between hydrophilic silica surface and DMPC membranes by using molecular dynamics (MD) simulations. The MD simulation has been successful simulate the similar system [58, 60]. We captured the force-distance profiles by running simulations varying lipid-substrate distances, calculated the diffusion coefficients of water under different systems, and analyzed the orientation of surface head-groups to investigate the polar properties' change, then compared results with experimental data, to see how the structure and dynamics properties of bilayer and interface water will be affected by hydrophilic substrate.

2. Simulation Methodology

2.1 Molecular Dynamics simulations

Molecular Dynamics is an important simulation method, bridging microscopic and macroscopic world together. The main different between MD simulation and other simulation methods is that MD focuses on the properties of molecules, exams the interaction between atoms-atoms, molecules-molecules in terms of body-body and provides a more detail and clear insights to the dynamical properties of the system. The equilibrium and dynamics of the systems are based on the calculation of time dependent physical movements of atoms according to Newton's equations.

$$F_i = m_i \frac{\partial^2 r_i}{\partial t^2} = -\frac{\partial U}{\partial r_i} \qquad \textit{Eq 2.1.1}$$

Where F_i is the force act on particle i, m_i is the mass of the particle, r_i is the position of particle i, U is the potential energy. From this equation, one can understand that potential energy should be a function of atomic positions, which can be shown as $U(r^N)$.

For a given system, the potential energy can be defined as the sum of non-bonded potential and bonded potential terms:

$$U = U_{bonded} + U_{non-bonded} \qquad \textit{Eq 2.1.2}$$

$$U_{bonded} = U_{bond} + U_{angle} + U_{dihedral} \qquad \textit{Eq 2.1.3}$$

$$U_{nonbonded} = U_{elec} + U_{vdW} \qquad \textit{Eq 2.1.4}$$

2.2 Force Field

Force field in molecular simulation specifies the energy functions form and parameters using to calculate the potential energy. There are many popular force fields, such as Amber, CHARMM， OPLS， CVFF and so on. However, each force field has its own target systems. For AMBER, it is mainly used to study protein and DNA system; For GROMOS, it is always used to study the bimolecular systems; OPLS, limited to be used in the liquid system. Among these force fields, CHARMM do not have much limitation, the simple form of function leads to a wide application: it can study both small molecules and macromolecules. In our study, we will use CHARMM force field to simulate the SBLs system.

In CHARMM force field, non-bonded potentials can be specified as the pair potential of atoms that are separated by more than two covalent bonds. Generally, it accounts to two kind of potentials: one is van der Waals (*Eq 2.2.1*), in which r_{ij} is the distance between atoms i and j, σ_{ij} is the effective atom diameter at which the inter-particle potential is zero, ε_{ij} is the Lennard-Jones parameters which defines the depth of potential well，all these parameters can be used to fit the experimental result; Another one is electrostatic interactions, in CHARMM force field, it can be described as coulomb potential (Eq 2.2.2), in which q_i and q_j are the charge of atoms i and j.

$$U_{lj} = \sum_{non-boonded} 4\varepsilon_{ij}\left[\left(\frac{\sigma_{ij}}{r_{ij}}\right)^{12} - \left(\frac{\sigma_{ij}}{r_{ij}}\right)^{6}\right] \qquad \textit{Eq 2.2.1}$$

$$U_{el} = \sum_{non-bonded} \frac{q_i q_j}{4\pi\varepsilon_o r_{ij}} \qquad \textit{Eq 2.2.2}$$

For bonded potential, it describes the vibration of bonds and bond angles, and bond rota-

tions in a molecule.

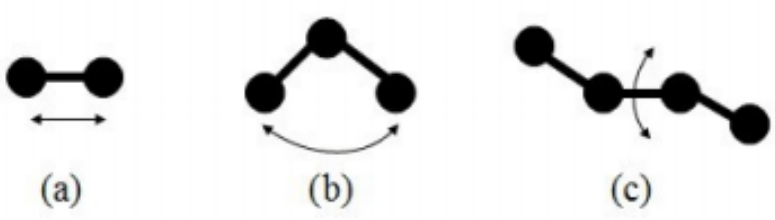

Fig 2-2-1. Schematic of vibration of bonds, angles and bond rotation

Eq. 2.2.3 and Eq.2.2.4 represent the harmonic potential of bonded atoms. The parameters k_b,k_θ are the force constants, r_0, $\theta_0$are the equilibrium bond distance and equilibrium angle . Eq. 2.2.5 describes the torsion angle potential, in which ϕ defines the torsion angle, $K_\emptyset$ is the force constant.

$$U_{harm}(r) = k_b(r - r_0)^2 \qquad \textit{Eq. 2.2.3}$$

$$U_{ang}(r) = k_\theta(\theta - \theta_0)^2 \qquad \textit{Eq. 2.2.4}$$

$$U_{tors}(\emptyset) = K_\emptyset(1 + \cos(M\emptyset - \Delta)) \qquad \textit{Eq. 2.2.5}$$

2.3 Building the model of silica substrate

To create a model of adsorbent, we constructed a slab-shaped block of amorphous silica. A cristobalite rectangular periodic system of 51.7Å x 51.7Å x 51.7Å was created using Materials Studio crystal builder and cleaved to make a 51.7Å x 51.7Å x 30Åslab. Then channels, or holes of about 6~8A in radius were created by removing some atoms. Hydroxyl groups were added manually to make a well hydroxylated surface with 4 OH groups per nm^2according to Katoh, [65] and then the loose ends were manually tied up. The block was melted in NVT MD simulations at 4000K with Morse potential [66] for 40ps, and then annealed to ambient temperature for 300ps. After equilibrium 30ps with normal pressure, we used CHARMM force field [67] and a standard Nose thermostat, to equilibrium the system for 100ps and a slab-shaped amorphous silica block emerged as a result. The slab is periodic on x-y plane, and non-periodic n z direction.

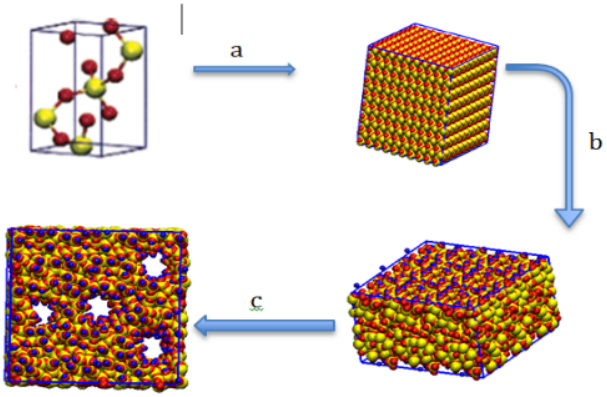

Figure 2-3-1. A) Building silica substrate.(a) A crystoballite unit cell was replicated, building a block size 51.7Å×51.7Å×51.7Å.(b)To obtain amorphous bulk and hydrophilic surface, the crystalline silica was cleaved to 51.7Å×51.7Å×30.0Å, add hydroxyl group on the surface manually, then increasing the temperature to 4000 K and then lowering it back to 300 K. (c) (d) Drilling four silica pores with 6~8Å radius (black circle), in order to let water easily go through the substrate, with little effect on the bilayer. The structure was annealed to produce silica pores.

2.4. Simulation details

In this study, the simulations were carried out using LAMMPs simulation software. All-atom CHARMM force field has been used to describe dimyristoylphosphatidylcholine (DMPC) [68] and hydrophilic silica substrate [67]. The water molecules are described by SPC model [69]. The lipid and silica were hydrated with 8139 water molecules, giving a total system size of ~40203 atoms. The simulation was carried out under conditions of constant volume and temperature of (303 K). Three-dimensional periodic boundary conditions were applied and long-range electrostatics computed with the particle mesh Ewald summation.

Initially, the DMPC bilayer are placed 30A from the silica substrate. In order to

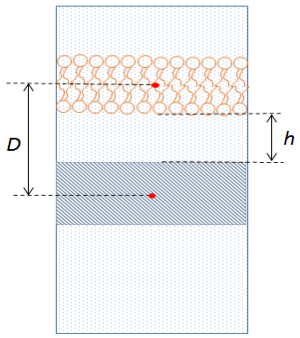

Fig 2-4-1 Schematic configuration of the model system. Orange part is lipid bilayer, grey part is substrate. d represent the distance between substrate-membrane center of mass

change the separation distance between bilayer and substrate, a gravity-type hydrostatic force is applied to both bilayer and water molecules after the previous system equilibrium. Three anchors were placed under the substrate to stabilize the substrate. The anchors were built of pseudo atoms that interacted only with the silica substrate and did not affect lipid molecules or water (shown as Fig 2-4-1).

Due to the gravity-type forces, the bilayer starts moving in z direction after a simulation start. The SLB moves until the system reaches equilibrium: that is, the gravity type force is counterbalanced by a disjoining force. Then the distance between the SLB and the silica block only fluctuates around a constant value (see Fig.2-4-1). The average distance over the stable part of the trajectory is used in the calculation of $f(D)$ and the structural properties. The equilibration part is discarded.

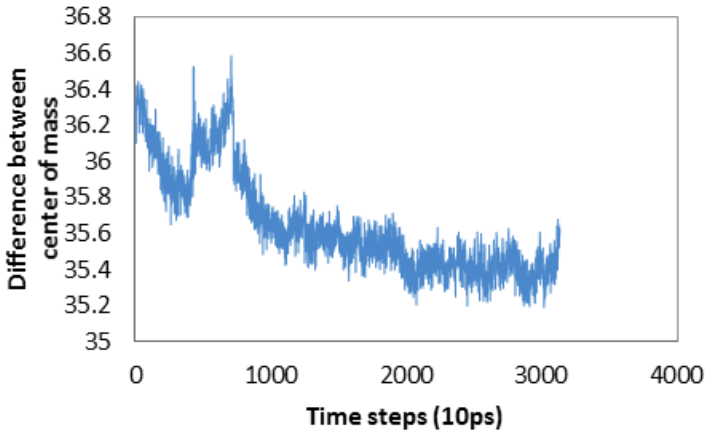

Fig. 2-4-1 Distance between center of mass of substrate and bilayer change with time steps. The separation of center mass of substrate and bilayer was fluctuated at large rage at fist 10 ns, after that the fluctuation tends to be flattening, around 35.4Å

The magnitude of the driving field g determines the total force driving the SLB towards (or away if g<0) to the substrate. The total driving force that is counterbalanced by the disjoining force

$$f(D) = g\sum_i m_i = \Pi(D) \times A \qquad \text{Eq. 2.4.1}$$

Where A is the surface, D is the distance between the centers of mass of the substrate and lipids, m_i are the masses of atoms to which the driving field is applied.

3. Results

3.1 SLB – Substrate Interaction Force

Systems with thin films are often having several types of equilibrium states, which can be stable, metastable or unstable. Two simulations with the same external field started from different initial configurations may come to different final configurations. Therefore, different types of states should be carefully probed. First, we started simulations from a configuration with about 30Å water layer between the SLB and the substrate with $g = 0$ (no external field applied). The system reaches equilibrium after 10ns. The final configuration is shown in Fig. 3-1-1. SLB and substrate are separated by a gap spacing of 27Å. This distance is in good agreement with the experimental data. [5, 68]. The disjoining pressure for such a configuration is zero.

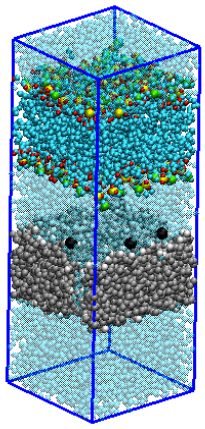

Fig. 3-1-1. Simulation snapshot with a 27Å gap separation between the lipid bilayer and silica substrate. Nitrogen and phosphorus atoms of the head groups are shown in yellow and green, respectively. The carbon atoms of the lipids chain are colored as cyan. Water molecules are transparent in the system, which are colored as blue. Silica substrate is grey, with hydrogen of hydroxyl on the surface being white.

The effective thickness of water layer can be calculated as the following process: integrate the density profile of water molecules, obtain the surface per mass of water, and then divide by the density of bulk water. On Fig 3-1-2, this first configuration with $\Pi = 0$ is shown as configuration is shown as point A. Starting from this configuration, we increased and decreased *g*, step by step. After *g* changes, the bilayer starts moving towards (if *g* increases) or away from the substrate (if *g* decreases). Typically, 10 ns were sufficient to establish the equilibrium with new *g*. By doing so, we have obtained a stable trajectory of A –type (Figure 3-2-1) configurations, which are characterized by Π ranging from 0.5kbar to 3kbar and correspondingly h ranging from 3.67 Å to 2.95 Å.

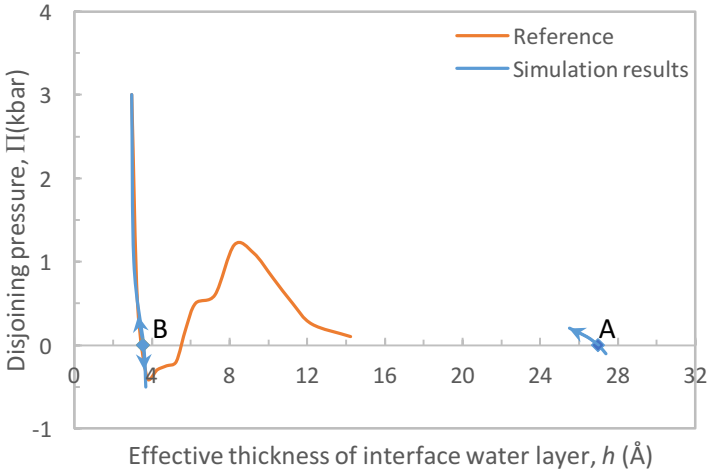

Fig. 3-1-2. Disjoining Pressure-effective thickness of water layer. Blue line is our simulation results; orange line is the simulation results from Pertsin et al[61].

A–type configurations are characterized by relatively weak attractions (which corresponds to weak attractions (positive Π) and weak repulsions (negative Π) as the thickness of water layer ranges from 26.5Å to 27.4Å. It is also clear that there exists another type of stable configurations with narrower water films. We will call them configurations of type B. For example, with g=0.18 kcal/(mol·Å) that corresponds to Π= 0.1kbar, is applied to the system, the separation distance between the center of mass of substrate and bilayer, denoted by d, will equilibrate around a constant value for about 20ns (shown as Fig3-1-3-b, yellow and grey line), and then will start irreversibly decreasing, and no stable configuration is reached within any reasonable simulation time. When *g* is greater than 0.18 kcal/(mol·Å) the bilayer will not be able to sustain the original separation distance, but rather immediately rush towards the substrate. We therefore conclude that B configurations are more stable than A (have generally lower free energy *G*) and are separated from them by a potential barrier that depends on *g*. The barrier is not overcome at lower *g*, but becomes low enough to be overcome due to thermal fluctuations at higher *g*. For higher Π, there exists no metastable configuration of A type.

Similar situation is observed when g decreases. Stable A-type films are observed with attraction between SLB and substrate g> 0.18 kcal/(mol·Å) which corresponds to Π>0.1kbar. If the attraction becomes stronger, the SLB starts an irreversible motion away from the substrate.

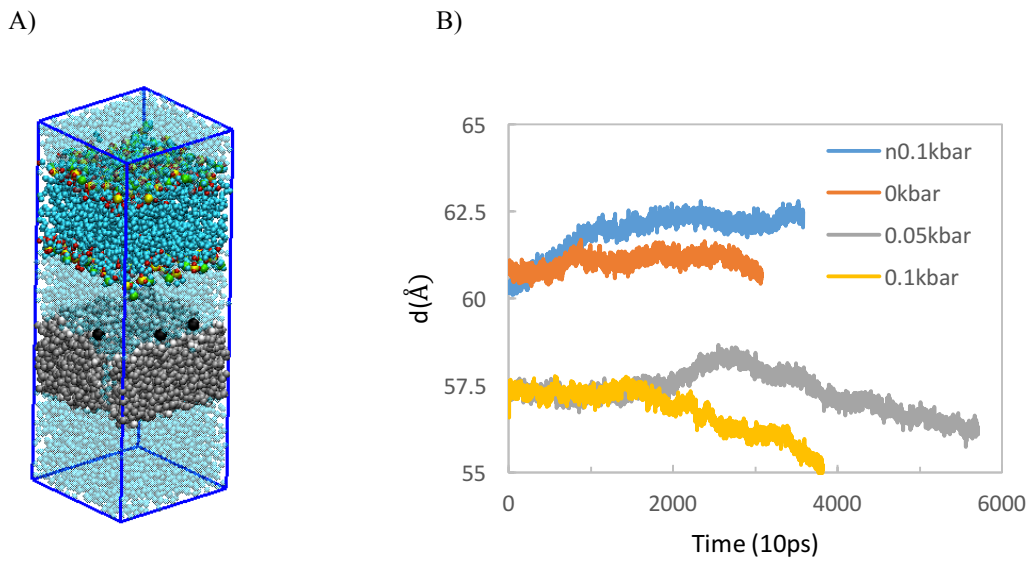

Fig 3-1-3. A) Snapshots of whole system with thick water layer at substrate-membrane interface. B) Separation between center of mass vs. time steps profile; when the system is under 0kbar, after 10ns running, the system will tend to reach equilibrium; but when applied a pressure of 0.05kbar or 0.1kbar, the system will equilibrium initially, then will make membrane move towards the substrate.

We should note that previous simulations [61] did not observe any configurations where a SLB separated by a substantial distance from the substrate experienced attraction to the latter. The authors assumed that on a long range, the SLB and mica surface experience a weak repulsion asymptotically decaying to 0 at h increases. In reality, that work only considered relatively small distances (Fig 3.1.2 orange line). Two hydrophilic monolayers, however, have been shown to attract on large h, and no configuration with several nm water film between the monolayer that corresponded to repulsion between them were obtained. In ref [60], MD simulation did show A-type configuration between DPPC and silica, although $\Pi(h)$ dependence was not studied. The distance between the substrate and the SLB at $\Pi = 0$ agrees very reasonably with experiment [68] where water film of 20A was observed in a similar system. Long distance attractions were also observed by both AFM and SPA experiments, and the attraction can be lasted till separation of bilayer and

substrate become 20nm. Due to the lower resolution of experimental equipment, short distance fluctuation of force cannot be obtained. From this point view, the existence of these long distance untestable configurations with attractive forces is reasonable.

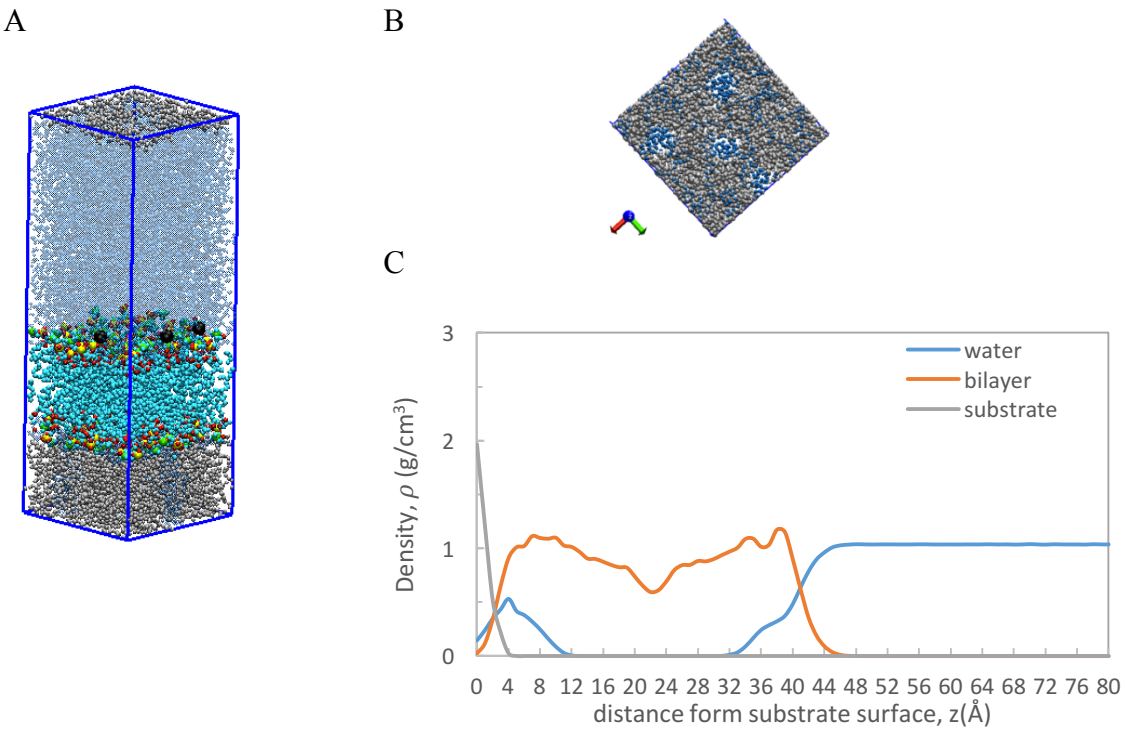

Fig 3-1-4. A) Snapshot of the total system with narrow water layer. B) A plan view of the substrate surface: the blue particles are the oxygen atoms of water molecules, the grey particles are the silica substrate, which are covered by lipid molecules (make the bilayer invisible). From this plan view, we can see that the water molecules do not cover the whole surface as a singular layer. C) Average density profile of the system without any external forces for B-type

B-type configurations were obtained by starting simulations with $g = 0$ and smaller h. In the process of simulation the SLB approached the substrate. Evaluation of the effective thickness of the water film between the SLB and substrate from the density profiles given in Fig 3-1-2 gives 3Å, which means that the film capacity if close to that of a monolayer of water molecules. In reality the density profiles for lipids and substrate partially over-

lap, and the snapshot given in Fig 3-1-4 shows that the bilayer in this configuration directly contacts the substrate, and only pockets of water remain. The interactions between the substrate and SLB are dominated by the hydrogen bonds that form between the lipid heads (as phosphate and carboxyl oxygens are hydrogen bond acceptors) and silica substrate (the hydroxyl donate those hydrogen bonds to lipids) as well as by van der Walls forces. If *g* increases, the lipid bilayer center of mass gets closer to the substrate. The $d\Pi/dh$ derivative is very high dues to steric repulsion between the lipids and silica. If *h* increases, the SLB and substrate attract, due to vdW attraction and the hydrogen bonds. Besides van der Waals repulsion and steric pressure, several other pressures are also possibly governing the short-range interactions [41]. Hydration pressure, for instance, exists when ordered water layers are formed under the influence of a hydrophilic head group of lipids and the hydrophilic solid surface

Pertsin et al [61] do not give a detailed account on the structure of substrate – SLB interface for this part of the trajectory. However, the analysis of their data also show that the water film corresponding to $\Pi = 0$ is extremely thin. If we overlap $\Pi=0$ points for their and our Π (*h*) curves, both sets of simulations give the same results for B-type configurations, at both positive and negative Π.

If g for B-type configurations is decreased below -0.9 kcal/(mol·Å), the driving field overpowers the substrate – SLB attraction, and the SLB starts irreversible motion away from the substrate. That is why we cannot obtain Π (*h*) for $\Pi < -0.5$ kbar. Obviously these states are thermodynamically unstable or metastable and close to the stability limit, so that a low potential barrier is overcome by thermal fluctuations.

Overall, we have determined two types of stable configuration: ones where SLB con-

tacts the substrate and those where they are separated by the water film of about 26A thick. We have to note that for stable configurations $(d\Pi/dh)_T < 0$. Since $\Pi = -dG/dh$, $d^2G/dh^2>0$, which is the main condition of the thermos dynamic stability of thin films. Configurations of B-type with a close contact between the substrate and SLB are dominated by the steric repulsion, vdW attraction and the direct hydrogen bond formation between the SLB and the substrate. In A-type configuration, the main forces are hydration forces, which are determined by the dependence of the free energy of water layer between SLB and substrate on h. For stable states $(d\Pi/dh)_T < 0$ (or $d^2G/dh^2 > 0$); stable regions A and B are separated by an interval of water film thicknesses where the films are unstable thermodynamically, $(d\Pi/dh)_T > 0$. We cannot exactly determine the limits of stability, because close to the limits the barrier for transitions are very low and are easily overcome by fluctuations that cause spontaneous changes of the configuration type. But our result suggest that qualitatively, $\Pi(h)$ dependence for DMPC SLB on silica can be described by a scheme shown in Figure 3-1-5. That is, as h increases, the steric repulsion is replaced by short-range attraction of SLB to substrate, which followed by a range of unstable water films, and then by stable water films that are actually observed in experiments as a results of spontaneous vesicle adsorption and spreading on silica (so called water gap described in Section 2.3). At long range, SLB and silica weekly attract. This attraction is the interaction that drives spontaneous vesicle adsorption and spreading on silica glass in standard experiments.

Note that the limit of stability of B-type configurations when separation increases corresponds to more negative g compared to A-type configurations. That is why on reverse motion (when D increases) A-type configurations cannot be observed, but rather the

system jumps to configurations with macroscopic water films between the surfaces. Basically, all A configurations are unstable at the force which corresponds to the limit of stability of B-type. On the approach in the SFA experiments, the film should experience an irreversible jump from point 3 to point 1. The approximately 2nm "shoulder" on approach curves on Fig 1-1-1 may indicate that such a phenomenon is indeed observed in the experiments.

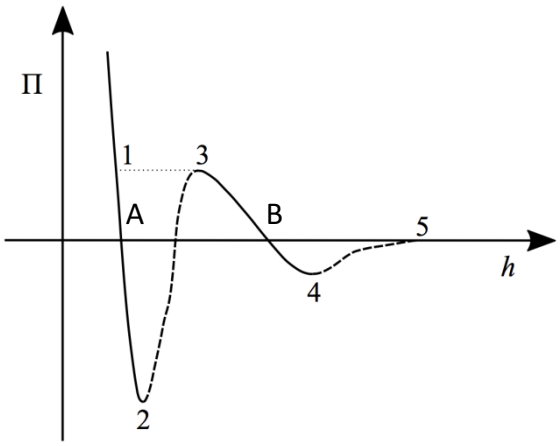

Fig 3-1-5 Qualitative schematics of disjoining pressure-dependence on distance between SLB and substrate. Solid lines represent the stable states and dotted lines represent the metastable states.

3.2 Characterization of the Structure

3.2.1 Orientation of Phosphatidylcholine Headgroups

The study of phosphatidylcholine group orientations can be interesting, since they could affect the electrostatic potential by reordering the dipole distribution. The orientation of headgroups are always described as the angle between the P to N vector and the normal vector of the bilayer surface, shown as Fig 3-2-1-A. An angle of 0° orientation corresponds to the case when vector P to N is perpendicular to the surface and pointing outwards from the bilayer; an angle of 90° orientation corresponds to the case when phosphatidylcholine head group is lying in the bilayer surface plane. The probability distributions of angles of upper leaflet and lower leaflet are calculated by averaging all the lipids of 20ns' trajectories, shown Fig 3-2-1. The distribution difference of upper and lower leaflets reveals the asymmetry of the bilayer, which is contributed by the existence of the silica substrate. For the upper leaflet, as the bilayer approaches the substrate the change in angular distribution can be negligible. For the lower leaflet, which is closer to the substrate, the change is significant. As shown in Fig3-2-1, the most probable values of θ are varied with each other: in the system with large separation (around position b), the most probable angle occurs around 88° and there is not much difference when the given forces are varied. In the system with a narrow water layer, the most probable angle occurs at 92° and a smaller peak was also observed at a range from 72° to 77°. As the separation becomes narrower, the smaller peak moves towards the large one, in other words, the headgroups will tend to be more parallel to the surface plane and the P to N vectors will more likely point towards the lipid tails. This can be understood when considering the hydrogen bonds. As the oxygen atoms of the phosphate groups are favorably

interacting with water molecules, the substrate-membrane interface becomes narrower, resulting in the hydrogen bonds becoming more complex and stronger as a consequence. This interaction will change the population distributions significantly.

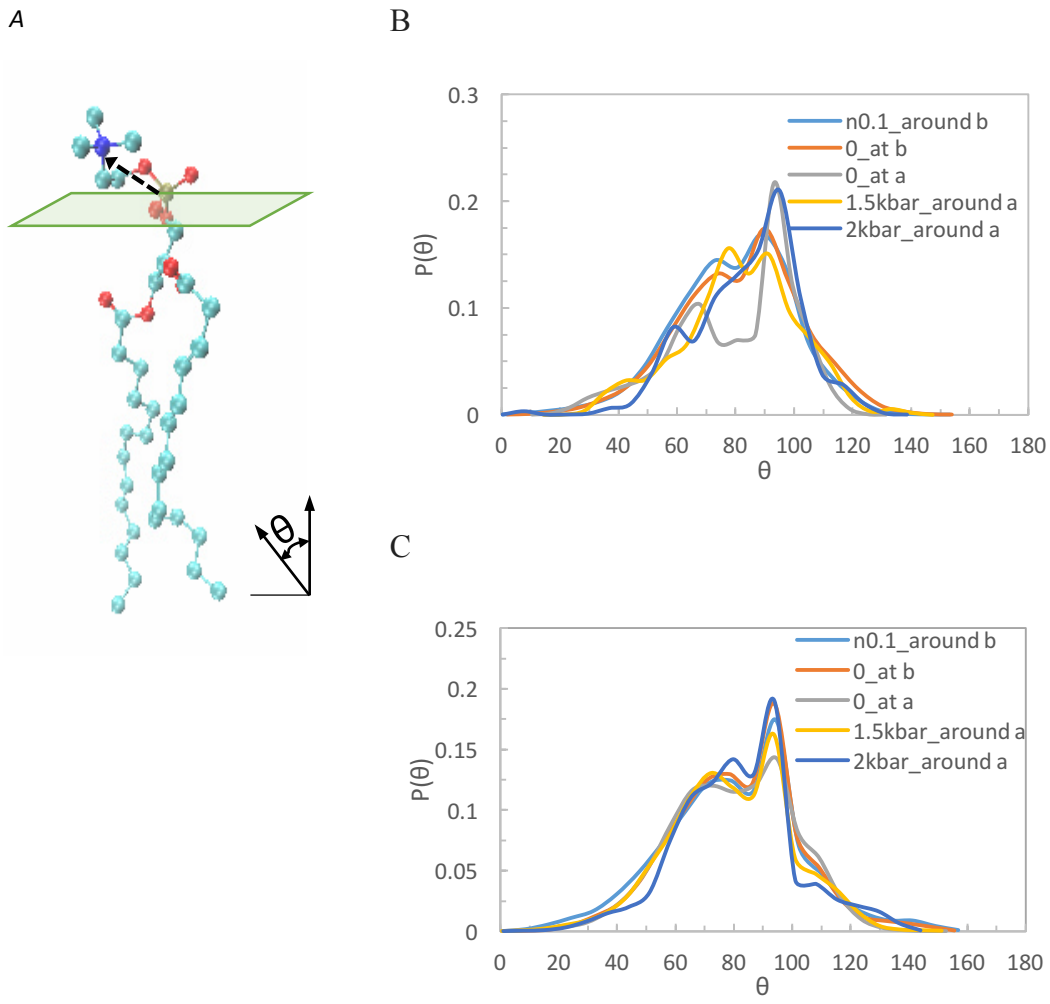

Fig 3-2-1 A) Schematic of orientation of Phosphatidylcholine head-groups; B) Angle distribution of lower leaflet; C) Angle distribution of upper leaflet

3.2.2 Order Parameters

In order to better understand the dynamics of lipids in bilayer and gain insights into the state of the system, order parameters were calculated. Order parameters are the most

popular quantities for characterizing the order in lipid bilayer, which can also be experimentally measured from NMR. It is defined as

$$S_{CD} = \frac{1}{2}\langle 3cos^2\theta - 1\rangle \qquad \textit{Eq 3.3.1}$$

Where θ is the angle between the C-H (or C-D in the case of NMR) vector and the membrane normal (Fig 3-3-1-A), brackets denote a time average. This parameter is a measure of the motional anisotropy of the particular C-H bond and yields its time-averaged orientation. If the chains are fixed in an all-trans conformation and are just rotating around the long molecular axis, the parameters would be -0.5; if a completely statistical movement through all angles of space occurs, then the parameters would be 0. This means the higher value of $-S_{CD}$ is, the more ordered the lipids will be. The order profile in Fig 3-3-1-B shows that the variation of the order parameter which is an expression of the average angular fluctuations around bilayer normal with position of the segment in the chain.

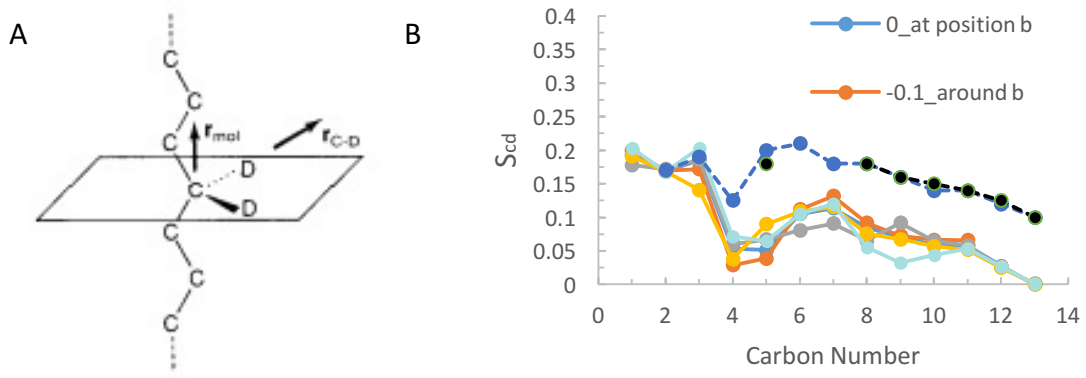

Fig 3-3-1 A) Schematic of the angle used for calculating S_{cd}; B) Deuterium order parameters for sn-1 chain

The simulation results are compared to both simulation and experimental data of free-standing DMPC bilayers. For the first and second carbon of sn2, the order parameter fits well with the data gained from reference[69]. For the other carbons, the order parameter is much lower, which means that the lipids will be more 'fluid' like because of the sub-

strate. In contrast, Chen et al[64] stated that the substrate's existence will make the proximal leaflet more ordering by giving the reason that the inner leaflet is under strong surface tension. They gave this conclusion by comparing the surface tension and density profile of supported DPPC bilayer system and free standing systems, but it is questionable to equate strong surface tension to a higher lipid order. In Kong's paper[70], they studied the effects of surface tension on lipid order, and made a conclusion that the increase in surface tension will make lipid tails become less ordered, especially under liquid crystal phase. To this extent, our results are in agreement with Chen's study: the substrate leads to a strong surface tension of inner leaflet and decreases the order parameter of the lipid chain.

In normal circumstances, the closer to the center of the bilayer, the value will be smaller, thus resulting in a larger mobility in the Carbon chain. It is interesting to obtain a curve structure with these peaks, but the reason is not clear. Similar curve structures were observed in the order profile of POPC bilayer, but they have a different condition: for POPC lipids, it contains double bonds in the hydrocarbon chain, so it is understandable some of the carbon will have a lower order parameters.

3.2.3 Diffusion coefficient of water

In the previous part, we studied how the substrate would affect the lipids structure of the bilayer, but the influence on the dynamic of water molecules is still not clear. Here, the lateral diffusion coefficients of bulk water and water molecules of interface layer are calculated by Einstein relation Eq 3.4.1.

$$D = \frac{\langle \left(\vec{r}(t_0 + t) - \vec{r}(t_0)\right)^2 \rangle}{4t} \qquad \textit{Eq 3.4.1}$$

Where $\langle(\vec{r}(t_0+t)-\vec{r}(t_0))^2\rangle$ is defined as MSD (mean square displacement). The calculation results were shown in Fig 3-4-1. The diffusion coefficient of bulk water is around $2.33\times10^{-5}cm^2s^{-1}$, which is in good agreement with the experimental results of $(2.34\pm0.05)\times10^{-5}cm^2s^{-1}$ at 298K, 1atm.[71] However, the diffusion of water molecules at the membrane-substrate interface is significantly impeded: when the substrate and bilayers have a short contact, the diffusion coefficient will be $(0.4\pm0.2)\times10^{-5}cm^2s^{-1}$. The small value suggests that the water molecules at the interface seem to have been 'blocked'; when the thickness of water layer is around 27Å, the diffusion coefficient is $(1.8\pm0.05)\times10^{-5}cm^2s^{-1}$. At short range some of lipids have been 'attached' to the surface and it is hard for water molecules to break out; however, when the separation become large, the effect of this kind of hydration force will be reduced and the 'mobility' of water molecules will be enhanced correspondingly. This similar phenomenon has also been observed in Carlos's paper [73]. In their paper[72], the interaction between water molecules and free standing DMPC bilayer has been studied, and the diffusion coefficient of water molecules associated with different region of lipids has also been calculated. The values are around$(1.9\pm0.4)\times10^{-7}cm^2s^{-1}$, suggesting that the water molecules are in a 'trapped' state at the surface of the membrane. In our system the existence of a substrate amplifies this effect.

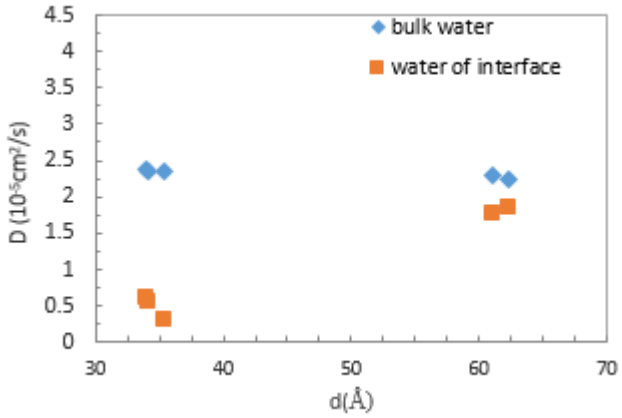

Fig 3-4-1 Diffusion Coefficient vs separation of substrate and bilayer.

3.2.4 Hydrogen Bond

To characterize the local structure and to quantify the interactions we calculate the number of hydrogen bonds in the selected system by using the geometrical criteria. The hydrogen bonds will be established when the distance between two oxygen atoms is less than 3.25Å and the angle of OHO is larger than 120° [73]. In our system not only water, but also the hydroxyl group dangling on the silica surface donates to the hydrogen bonds. There are several potential acceptors in the system including water, lipids tail oxygen, phosphorous group oxygen, and oxygen of hydroxyl group. The total number of H-bonds donated per water molecules decreases from 1.9 to 1.2 as the thickness of the water layer becomes smaller. The total number of H-bonds donated per hydroxyl group is close to 1, 70% of it will be accepted by water, and 20% will be accepted by the non-ester oxygen of phosphate groups. When the bilayer is pushed towards the substrate the proportion of H-bond with non-ester oxygen increases. This suggests that the phosphate groups are more likely to be exposed to substrate as the separation distance between bilayer and substrate become small, which is in agreement with the orientation of Phosphatidylcholine group.

3.2.5 Radial Distribution Functions

To better understand the interactions we computed the radial distribution functions (RDF). It can be defined as

$$g(r) = \frac{n(r, r + \Delta r)}{\rho \Delta V_{2D}} \qquad \textit{Eq 3.6.1}$$

where $\Delta V_{2D}$is the volume of a shell with radius r, $n(r, r + \Delta r)$ is the number of molecules in this shell, and ρ is the 2D density.

Fig 3-6-1 shows that RDF of water's oxygen atoms relative to different reference atoms and Fig 3-6-2 shows RDFs for oxygen of hydroxyl on substrate around other reference atoms. Only nitrogen and lipids oxygen atoms have been chosen to calculate the RDFs based on their ability to build hydrogen bonds with water and hydroxyl on the silica substrate. RDFs do not differ from the different disjoining pressure, we only show the RDFs results of the system without applying any pressures.

Multiple interaction shell can be observed from the RDFs of water's hydrogen to lipid phosphate's oxygen and of water oxygen's to lipid's nitrogen. In the case of phosphate oxygen-water RDF (shown in Fig 3-6-1-A), the multiple peaks demonstrate a significant and complex interaction exists between phosphorus group and water molecules. From the RDFs and SDF-surface density functions (Fig 3-6-1-B), we can see that there are generally two water molecules surround the phosphorous groups that bond to the non-ester oxygen of phosphate group. From Fig3-6-1-B, we see that the existence of a further shell that suggests there should be a hydrogen bridge around the ester oxygen, which is close to the nitrogen group. It is possible that there will be a third water bonding to the water's bonded to non-ester phosphate oxygen for the hydrogen bonding bridge.

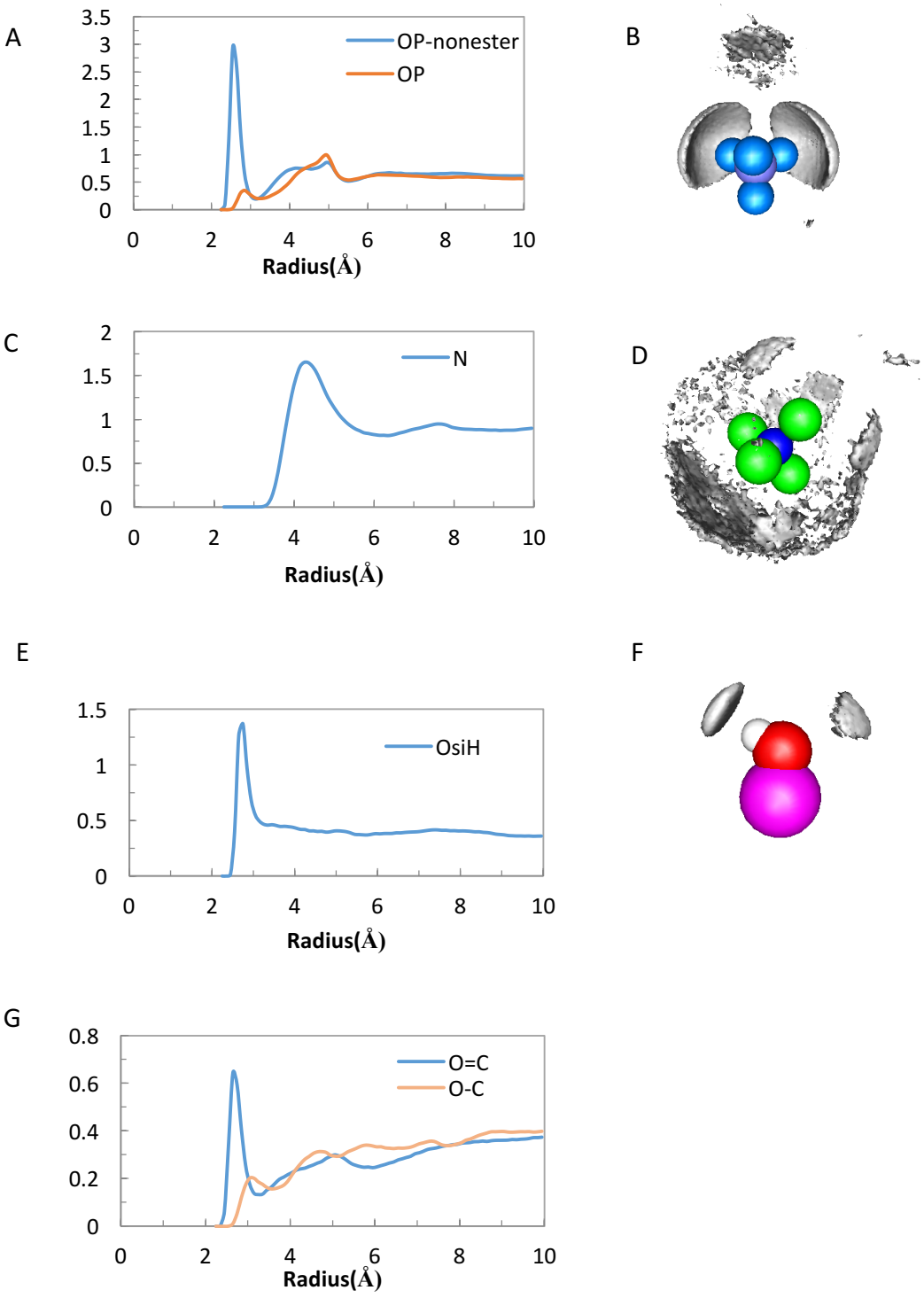

Fig 3-6-1. RDFs and SDFs for water around different refrence atoms: A) and B) phosphate oxygen; C) and D) Choline Nitrogen; E) and F) hydroxyl oxygen of Silica; G) tail oxygen atoms.

The choline nitrogen-water RDF is shown in Fig 3-6-1-C. The largest peak is at 4.25Å and the next peak with shoulder is at 7.75Å, which indicates a highly-defined solvation structure surrounding the choline group and even though nitrogen cannot form hydrogen bonds with the water directly. In SDF (Fig 3-6-1-D) higher density will be found around three methyl groups.

For the oxygen of lipid tail (Fig 3-6-1-G), the average density distribution is much lower when compared to other atoms' RDFs, even though the solvation shell can also be observed. These results are in agreement with the all-atom molecular dynamics calculations of Lopez et al[72], using the AMBER force field with SPC/E water as solvent.

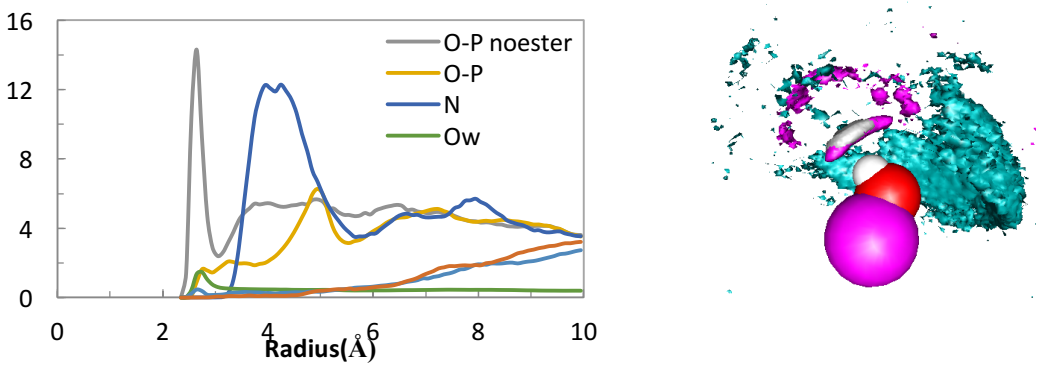

Fig 3-6-2 RDFs and SDF for hydroxyl oxygen around different reference atoms

In order to explore the interaction between lipid and water, RDFs for hydroxyl oxygen of substrate around lipids reference atoms have been calculated with a very narrow water-membrane interface (Fig 3-6-2). These structural features are similar to water based RDFs.

4. Conclusion

We studied the interaction between DMPC lipids bilayer and hydrophilic silica substrate. A new model for atomistic simulation of supported bilayer has been proposed. Detailed construction has been discussed in Section 2. In our model, instead of varying distance of the gap region by adding or taking off water molecules manually[58] , we applied a different size of gravity-like force, corresponds to different size of disjoining pressure, to the lipids and water molecules to obtain the corresponding equilibrium separations. In this way disjoining pressure vs separation curve has been captured. The interesting part is without applying any force, we achieved two different equilibrium separations, one of them is at a very short distance and the other one is with about 25Å thickness of water layer. The sigmoidal shape of pressure-distance curve shows that there are at configurations with attractive disjoining pressure.

As the separation between substrate and bilayer decreases, the head-group will be preferable parallel to the bilayer surface. This may be caused by the strong hydrogen bonds between the phosphate groups and hydroxyl on the silica substrate, which is in good agreement with the hydrogen bond probabilities and radial distribution functions. The dynamics of water molecules at interface were studied by comparing the diffusion coefficient with bulk water, by analyzing the probabilities of hydrogen bonds creation, and by calculating the radius distribution functions. The water at the interface has a lower diffusion coefficient and a higher possibility to create hydrogen bonds with phosphate groups.

Although only two branches of force-separation curve have been measured based on the analysis above, it's very possible that the curve may have an oscillating structure, which may contain several metastable states.

5. References

1. Castellana, E.T. and P.S. Cremer, *Solid supported lipid bilayers: From biophysical studies to sensor design.* Surface Science Reports, 2006. **61**(10): p. 429-444.
2. Groves, J.T. and M.L. Dustin, *Supported planar bilayers in studies on immune cell adhesion and communication.* Journal of Immunological Methods, 2003. **278**(1-2): p. 19-32.
3. Knoll, W., et al., *Solid supported lipid membranes: New concepts for the biomimetic functionalization of solid surfaces.* Biointerphases, 2008. **3**(2): p. Fa125-Fa135.
4. Richter, R.P., R. Berat, and A.R. Brisson, *Formation of solid-supported lipid bilayers: An integrated view.* Langmuir, 2006. **22**(8): p. 3497-3505.
5. Sackmann, E., *Supported membranes: Scientific and practical applications.* Science, 1996. **271**(5245): p. 43-48.
6. Shen, S.K., et al., *Liposil-supported lipid bilayers as a hybrid platform for drug delivery.* Soft Matter, 2011. **7**(3): p. 1001-1005.
7. Tero, R., *Substrate Effects on the Formation Process, Structure and Physicochemical Properties of Supported Lipid Bilayers.* Materials, 2012. **5**(12): p. 2658-2680.
8. Kim, J., G. Kim, and P.S. Cremer, *Investigations of water structure at the solid/liquid interface in the presence of supported lipid bilayers by vibrational sum frequency spectroscopy.* Langmuir, 2001. **17**(23): p. 7255-7260.
9. Kiessling, V. and L.K. Tamm, *Measuring distances in supported bilayers by fluorescence interference-contrast microscopy: Polymer supports and SNARE proteins.* Biophysical Journal, 2003. **84**(1): p. 408-418.
10. Crane, J.M., V. Kiessling, and L.K. Tamm, *Measuring lipid asymmetry in planar supported bilayers by fluorescence interference contrast microscopy.* Langmuir, 2005. **21**(4): p. 1377-1388.
11. Watkins, E.B., et al., *Structure and Orientational Texture of Self-Organizing Lipid Bilayers.* Physical Review Letters, 2009. **102**(23).
12. Johnson, S.J., et al., *Structure of an Adsorbed Dimyristoylphosphatidylcholine Bilayer Measured with Specular Reflection of Neutrons.* Biophysical Journal, 1991. **59**(2): p. 289-294.
13. Feng, Z.V., T.A. Spurlin, and A.A. Gewirth, *Direct visualization of asymmetric behavior in supported lipid bilayers at the gel-fluid phase transition.* Biophysical Journal, 2005. **88**(3): p. 2154-2164.
14. Rossetti, F.F., M. Textor, and I. Reviakine, *Asymmetric distribution of phosphatidyl serine in supported phospholipid bilayers on titanium dioxide.* Langmuir, 2006. **22**(8): p. 3467-3473.
15. Shreve, A.P., et al., *Evidence for Leaflet-Dependent Redistribution of Charged Molecules in Fluid Supported Phospholipid Bilayers.* Langmuir, 2008. **24**(23): p. 13250-13253.
16. Stanglmaier, S., et al., *Asymmetric Distribution of Anionic Phospholipids in*

Supported Lipid Bilayers. Langmuir, 2012. **28**(29): p. 10818-10821.
17. *IUPAC Compendium of Chemical Terminology-"The Gold Book"*. 1997; 2nd [
18. McNamee, C.E., et al., *Interfacial Forces between a Silica Particle and Phosphatidylcholine Monolayers at the Air-Water Interface.* Langmuir, 2010. **26**(18): p. 14574-14581.
19. Gong, X.J., Z.H. Wang, and T. Ngai, *Direct measurements of particle-surface interactions in aqueous solutions with total internal reflection microscopy.* Chemical Communications, 2014. **50**(50): p. 6556-6570.
20. Burnham, N.A., et al., *Probing the Surface Forces of Monolayer Films with an Atomic-Force Microscope.* Physical Review Letters, 1990. **64**(16): p. 1931-1934.
21. Butt, H.J., *Measuring Electrostatic, Vanderwaals, and Hydration Forces in Electrolyte-Solutions with an Atomic Force Microscope.* Biophysical Journal, 1991. **60**(6): p. 1438-1444.
22. Anderson, T.H., et al., *Direct Measurement of Double-Layer, van der Waals, and Polymer Depletion Attraction Forces between Supported Cationic Bilayers.* Langmuir, 2010. **26**(18): p. 14458-14465.
23. Valtiner, M., et al., *Hydrophobic Forces, Electrostatic Steering, and Acid-Base Bridging between Atomically Smooth Self-Assembled Monolayers and End-Functionalized PEGolated Lipid Bilayers.* Journal of the American Chemical Society, 2012. **134**(3): p. 1746-1753.
24. Anderson, T.H., et al., *Formation of Supported Bilayers on Silica Substrates.* Langmuir, 2009. **25**(12): p. 6997-7005.
25. Michael V. Rapp, S.H.D., Jr.,† Matthew A. Gebbie,‡ Yonas Gizaw, § Peter Koenig, // and a.J.N.I. Yuri Roiter, *Effects of Surfactants and Polyelectrolytes on the Interaction between a Negatively Charged Surface and a Hydrophobic Polymer Surface.* Langmuir, 2015.
26. Yu, J., et al., *Adaptive hydrophobic and hydrophilic interactions of mussel foot proteins with organic thin films.* Proceedings of the National Academy of Sciences of the United States of America, 2013. **110**(39): p. 15680-15685.
27. Stephen H. Donaldson, J.a., et al., *General hydrophobic interaction potential for surfactant/lipid bilayers from direct force measurements between light-modulated bilayers.* PNAS, 2011. **108**.
28. Donaldson, S.H., et al., *Asymmetric Electrostatic and Hydrophobic-Hydrophilic Interaction Forces between Mica Surfaces and Silicone Polymer Thin Films.* Acs Nano, 2013. **7**(11): p. 10094-10104.
29. Israelachvili, J.N., *Intermolecular and Surface Forces*. Third edition ed. 2011.
30. O'shea, S.J., et al., *Liquid Atomic Force Microscopy: Solvation Forces, Molecular Order, and Squeeze-Out.* Japanese Journal of Applied Physics, 2010. **49**(8).
31. Lim, R., S.F.Y. Li, and S.J. O'Shea, *Solvation forces using sample-modulation atomic force microscopy.* Langmuir, 2002. **18**(16): p. 6116-6124.
32. Steltenkamp, S., et al., *Mechanical properties of pore-spanning lipid bilayers probed by atomic force microscopy.* Biophysical Journal, 2006. **91**(1): p. 217-226.
33. Alessandrini, A., et al., *What do we really measure in AFM punch-through experiments on supported lipid bilayers?* Soft Matter, 2011. **7**(15): p. 7054-7064.

34. Alessandrini, A. and P. Facci, *Nanoscale mechanical properties of lipid bilayers and their relevance in biomembrane organization and function.* Micron, 2012. **43**(12): p. 1212-1223.
35. Li, J.K., R.M.A. Sullan, and S. Zou, *Atomic Force Microscopy Force Mapping in the Study of Supported Lipid Bilayers.* Langmuir, 2011. **27**(4): p. 1308-1313.
36. Frisbie, C.D., et al., *Functional-Group Imaging by Chemical Force Microscopy.* Science, 1994. **265**(5181): p. 2071-2074.
37. Das, C., et al., *Nanoscale mechanical probing of supported lipid bilayers with atomic force microscopy.* Physical Review E, 2010. **82**(4).
38. Schneider, J., W. Barger, and G.U. Lee, *Nanometer scale surface properties of supported lipid bilayers measured with hydrophobic and hydrophilic atomic force microscope probes.* Langmuir, 2003. **19**(5): p. 1899-1907.
39. Abdulreda, M.H., et al., *Pulling force generated by interacting SNAREs facilitates membrane hemifusion.* Integrative Biology, 2009. **1**(4): p. 301-310.
40. Abdulreda, M.H. and V.T. Moy, *Atomic force microscope studies of the fusion of floating lipid bilayers.* Biophysical Journal, 2007. **92**(12): p. 4369-4378.
41. Israelachvili, J.N. and H. Wennerstrom, *Entropic Forces between Amphiphilic Surfaces in Liquids.* Journal of Physical Chemistry, 1992. **96**(2): p. 520-531.
42. Pera, I., et al., *Using the atomic force microscope to study the interaction between two solid supported lipid bilayers and the influence of synapsin I.* Biophysical Journal, 2004. **87**(4): p. 2446-2455.
43. Lipowsky, R. and S. Grotehans, *Hydration Vs Protrusion Forces between Lipid Bilayers.* Europhysics Letters, 1993. **23**(8): p. 599-604.
44. Argyris, D., P.D. Ashby, and A. Striolo, *Structure and Orientation of Interfacial Water Determine Atomic Force Microscopy Results: Insights from Molecular Dynamics Simulations.* Acs Nano, 2011. **5**(3): p. 2215-2223.
45. Asakawa, H., et al., *Spatial Distribution of Lipid Headgroups and Water Molecules at Membrane/Water Interfaces Visualized by Three-Dimensional Scanning Force Microscopy.* Acs Nano, 2012. **6**(10): p. 9013-9020.
46. Fukuma, T., *Water distribution at solid/liquid interfaces visualized by frequency modulation atomic force microscopy.* Science and Technology of Advanced Materials, 2010. **11**(3).
47. Higgins, M.J., et al., *Structured water layers adjacent to biological membranes.* Biophysical Journal, 2006. **91**(7): p. 2532-2542.
48. Jackman, J.A., et al., *Self-Assembly Formation of Lipid Bilayer Coatings on Bare Aluminum Oxide: Overcoming the Force of Interfacial Water.* Acs Applied Materials & Interfaces, 2015. **7**(1): p. 959-968.
49. Parikh, A.N., *Membrane-substrate interface: Phospholipid bilayers are chemically and topographically structured surfaces.* Biointerphases, 2008. **3**(2): p. Fa22-Fa32.
50. Nussio, M.R., et al., *Nanomechanical Characterization of Phospholipid Bilayer Islands on Flat and Porous Substrates: A Force Spectroscopy Study.* Journal of Physical Chemistry B, 2009. **113**(30): p. 10339-10347.
51. Andreas Janshoff, C.S., *Mechanics of lipid bilayers: What do we learn from pore-*

spanning membranes? Biochimica et Biophysica Acta (BBA) 2015.
52. Guardingo, M., et al., *Bioinspired Catechol-Terminated Self-Assembled Monolayers with Enhanced Adhesion Properties.* Small, 2014. **10**(8): p. 1594-1602.
53. Pujari, S.P. and H. Zuilhof, *Highly wear-resistant ultra-thin per-fluorinated organic monolayers on silicon(111) surfaces.* Applied Surface Science, 2013. **287**: p. 159-164.
54. Gosvami, N.N., et al., *Resolving the structure of a model hydrophobic surface: DODAB monolayers on mica.* Rsc Advances, 2012. **2**(10): p. 4181-4188.
55. Hiasa, T., K. Kimura, and H. Onishi, *Hydration of hydrophilic thiolate monolayers visualized by atomic force microscopy (vol 14, pg 8419, 2012).* Physical Chemistry Chemical Physics, 2013. **15**(48): p. 21097-21097.
56. Kim, H.I., et al., *How disjoining pressure drives the dewetting of a polymer film on a silicon surface.* Physical Review Letters, 1999. **82**(17): p. 3496-3499.
57. Ma, C.D., et al., *Modulation of hydrophobic interactions by proximally immobilized ions.* Nature, 2015. **517**(7534): p. 347-U443.
58. Heine, D.R., A.R. Rammohan, and J. Balakrishnan, *Atomistic simulations of the interaction between lipid bilayers and substrates.* Molecular Simulation, 2007. **33**(4-5): p. 391-397.
59. J.N. Israelachvili, Private communication
60. Matthew Roark and S.E. Feller, *Structure and Dynamics of a Fluid Phase Bilayer on a Solid Support as Observed by a Molecular Dynamics Computer Simulation.* Langmuir, 2008. **24**: p. 12469-12473.
61. Pertsin, A. and M. Grunze, *Possible mechanism of adhesion in a mica supported phospholipid bilayer.* Journal of Chemical Physics, 2014. **140**(18).
62. Xing, C.Y. and R. Faller, *Interactions of lipid bilayers with supports: A coarse-grained molecular simulation study.* Journal of Physical Chemistry B, 2008. **112**(23): p. 7086-7094.
63. Hoopes, M.I., et al., *Coarse-grained modeling of interactions of lipid bilayers with supports.* Journal of Chemical Physics, 2008. **129**(17).
64. Xing, C.Y., et al., *Asymmetric nature of lateral pressure profiles in supported lipid membranes and its implications for membrane protein functions.* Soft Matter, 2009. **5**(17): p. 3258-3261.
65. Katoh, M., et al., *Adsorption of CO2 on FSM-type mesoporous silicas.* Physical Chemistry Chemical Physics, 2000. **2**(19): p. 4471-4475.
66. Demiralp, E., T. Cagin, and W.A. Goddard, *Morse stretch potential charge equilibrium force field for ceramics: Application to the quartz-stishovite phase transition and to silica glass.* Physical Review Letters, 1999. **82**(8): p. 1708-1711.
67. Cruz-Chu, E.R., A. Aksimentiev, and K. Schulten, *Water-silica force field for simulating nanodevices.* Journal of Physical Chemistry B, 2006. **110**(43): p. 21497-21508.
68. Bayerl, T.M. and M. Bloom, *Physical-Properties of Single Phospholipid-Bilayers Adsorbed to Micro Glass-Beads - a New Vesicular Model System Studied by H-2-Nuclear Magnetic-Resonance.* Biophysical Journal, 1990. **58**(2): p. 357-362.

69. Kasson, P.M. and V.S. Pande, *Molecular dynamics simulation of lipid reorientation at bilayer edges.* Biophysical Journal, 2004. **86**(6): p. 3744-3749.
70. Kong, X., et al., *Surface tension effects on the phase transition of a DPPC bilayer with and without protein: a molecular dynamics simulation.* Physical Chemistry Chemical Physics, 2014. **16**(18): p. 8434-8440.
71. Wu, Y.J., H.L. Tepper, and G.A. Voth, *Flexible simple point-charge water model with improved liquid-state properties.* Journal of Chemical Physics, 2006. **124**(2).
72. Lopez, C.F., et al., *Hydrogen bonding structure and dynamics of water at the dimyristoylphosphatidylcholine lipid bilayer surface from a molecular dynamics simulation.* Journal of Physical Chemistry B, 2004. **108**(21): p. 6603-6610.
73. Lyubartsev, A.P. and A. Laaksonen, *Molecular dynamics simulations of DNA in solution with different counter-ions.* Journal of Biomolecular Structure & Dynamics, 1998. **16**(3): p. 579-+.